Published in final edited form as:
Genesis. 2009 July ; 47(7): 469–475. doi:10.1002/dvg.20524.

Generation of *Smad7*$^{-Cre}$ Recombinase Mice: A Useful Tool for the Study of Epithelial-Mesenchymal Transformation Within the Embryonic Heart

Paige Snider[1,*], **Sunyong Tang**[1,2], **Goldie Lin**[1], **Jian Wang**[1], and **Simon J. Conway**[1,2,3,4,*]

[1] Riley Heart Research Center, HB Wells Center for Pediatric Research, Indiana University School of Medicine, Indianapolis, Indiana

[2] Department of Biochemistry and Molecular Biology, Indiana University School of Medicine, Indianapolis, Indiana

[3] Department of Anatomy and Cell Biology, Indiana University School of Medicine, Indianapolis, Indiana

[4] Department of Medical and Molecular Genetics, Indiana University School of Medicine, Indianapolis, Indiana

Summary

Smad7 can be induced by various transforming growth factor-*β* superfamily ligands and negatively modulates their signaling, thus acting in a negative, autocrine feedback manner. Previous analyses have demonstrated that although Smad7 is widely expressed, it is predominantly found in the vascular endothelium. Because of the restricted spatiotemporal reporter expression driven via a novel 4.3 kb Smad7 promoter in endocardial cells overlying the hearts atrioventricular (AV) cushions; we hypothesized that a transgenic *Cre* line would prove useful for the analysis of endocardial cushion and valve formation. Here we describe a mouse line, *Smad7*^{Cre}, where Cre is robustly expressed within both cardiac outflow and AV endocardial cushions. Additionally, as endocardial cells are thought to contribute at least in part to the formation of the endocardial cushion mesenchyme, we crossed the *Smad7*^{Cre} mice to the *ROSA26*$^{eGFP\text{-}DTA}$ diphtheria toxin A-expressing mice in order to genetically ablate *Smad7*^{Cre} expressing cells. Ablation of *Smad7*^{Cre} cells resulted in embryonic lethality by E11.5 and largely acellular endocardial cushions.

Keywords

mouse embryo; Smad7; Cre recombinase; endocardial cushions; heart development; Cre/loxP cell ablation

Formation of the endocardial cushions is a key step in heart development, as the endocardial cushions are required for chamber septation, valve formation, and to sustain unidirectional blood flow and embryo viability (Schroeder *et al*., 2003). An important initiator event in endocardial cushion morphogenesis is epithelial-to-mesenchymal transformation (EMT), the process whereby overlying endocardial cells undergo rapid transformation into mesenchyme (de Lange *et al*., 2004; Eisenberg and Markwald, 1995; Kisanuki *et al*., 2001; Stevens *et al*., 2008). It is well established that members of the transforming growth factor-β superfamily

*Correspondence to: Paige Snider or Simon J. Conway, Conway Laboratory, 1044 West Walnut Street, Room R4 W379, Indiana University School of Medicine, Indianapolis, IN 46202, USA., psnider@iupui.edu or siconway@iupui.edu.

(TGFβ) play a role in the signaling from adjacent myocardium to the responding endocardium to begin EMT (Eisenberg and Markwald, 1995; Nakajima *et al*., 2000; Schroeder *et al*., 2003; Zhou *et al*., 2005).

The TGFβ superfamily of secretory polypeptides exert their biological function by binding to their cognate serine/threonine receptors to activate Smad proteins to regulate target gene expression (Massague *et al*., 2005). TGFβ signaling is important in a diverse group of cell types and regulates cell migration, differentiation, adhesion, proliferation, and apoptosis during embryonic development (Luukko *et al*., 2001; Massague and Wotton, 2000; Moustakas *et al*., 2001). Smad7 is an inhibitory Smad that blocks TGFβ signaling (Imamura *et al*., 1997; Nakao *et al*., 1997). Smad7 inhibits both TGFβ/activin and BMP signaling (Hayashi *et al*., 1997; Massague *et al*., 2005), via competitively inhibiting the activation of regulatory Smads (intracellular signal transducers) and promoting TGFβ receptor degradation (Kavsak *et al*., 2000; Massague *et al*., 2005). We generated a *Smad7*^{Cre} transgenic mouse line with Cre recombinase expression being driven by the novel 4.3 kb *Smad7* promoter (Liu *et al*., 2007), as a tool to assess both lineage derivatives and to study gene function during embryonic development. Additionally, by crossing this mouse line with the *ROSA26*$^{eGFP\text{-}DTA}$ mice (Ivanova 2009 Wiley-Liss, Inc. genesis 00:000–000 (2009) *et al*., 2005; Snider *et al*., 2008a), the Cre expressing cell lineages were genetically ablated with no bystander effects, in order to test the eventual requirement of the *Smad7*^{Cre} cell lineage in utero.

To determine *Smad7*^{Cre} spatiotemporal expression and its lineage mapping, we crossed *Smad7*^{Cre} with *ROSA26R lacZ* reporter (*R26r*) mice (Soriano, 1999). *LacZ* expression could initially be seen at E9.5 and by E10.5, the *Samd7*^{Cre}*;R26r* mice exhibited robust staining in ventral structures including the lower jaw, aortic arch arteries, heart, limb buds, and brain (Fig. 1a). Initial *lacZ* expression patterns were similar to those of endogenous *Smad7 mRNA* expression at these early ages (Luukko *et al*., 2001). *Smad7*^{Cre} driven *lacZ* reporter activity is present in E9.5 and older limbs, and is restricted to the ventral limb ectoderm and underlying mesoderm (histology not shown; Fig. 1a,c). The *lacZ* ectodermal expression pattern is similar to that observed for the homeodomain-containing *Engrailed-1* transcription factor, which is expressed within only the embryonic ventral limb ectoderm (Loomis *et al*., 1996). At E10.5, we see very robust expression in the endodermal epithelia of the branchial pouches of the third and fourth arch artery (Fig. 1i). Examination of the heart revealed robust expression in the outflow tract (OFT) and atrioventricular (AV) endocardial cushions with punctate staining within the myocardium (Fig. 1b). This cushion expression is much greater than that observed in 4.3 kb *Smad7*$^{-lacZ}$ reporter mice, due to our ability to mark both cells actively expressing Cre, and their daughter cells. Consequently, E11.5 embryos exhibit stronger (cumulative) *lacZ* staining in the heart, as well as the face, arches, limbs, eye, and brain (Fig. 1c). Embryos containing *R26r* but no Cre, do not exhibit any *lacZ* or background staining, even after several days in X-gal substrate (Fig. 1d). At E13.5, *lacZ* expression remains robust within the aorta and pulmonary vessels, atria, and punctate in the ventricle (Fig. 1e). *Smad7*^{Cre}*;R26r* reporter activity is now also observed in the ventral lung bud and midgut/dorsal mesentery tissues adjacent to dorsal aorta (Fig. 1f). Besides the robust reporter expression observed in the cardiovascular system, there was notable restricted *lacZ* in the entrance of optic stalk, neuroepithelial adjacent to hindbrain roof and telencephalic neuroepithelium at telencephalic-mesencephalic boundary (Fig. 1k). We also observed restricted *lacZ* staining in the eye (Fig. 1l,m).

Histological analysis of *lacZ*-stained E10.5 hearts revealed extensive *Smad7*^{Cre} positive endothelial cells in the conus, but fewer in the truncus of the OFT (Fig. 1g). Although the truncus is largely derived from neural crest, the distal conus is derived solely from endocardial EMT (de Lange *et al*., 2004;Kisanuki *et al*., 2001;Snider *et al*., 2007;Zhou *et al*., 2005). The endocardium of the AV cushions stains strongly for *lacZ*, although clearly not all endocardial

cells are Cre-positive (Fig. 1g). Additionally, the majority of the endocardial cells covering the trabeculae of the myocardium are also *lacZ* positive (Fig. 1h). Given that the 4.3 kb *Smad7*$^{-lacZ}$ reporter did not exhibit any ventricular endocardial expression (Liu *et al*., 2007), this enhanced *Smad7*^{Cre}*;R26r* reporter activity illustrates the sensitivity of the *LoxP/Cre* lineage marking recombination system. These data suggest that *Smad7*^{Cre} is likely transiently expressed early with little Cre, but that this is still sufficient to result in permanent endocardial cushion *lacZ* expression. Similar to the 4.3 kb *Smad7*$^{-lacZ}$ reporter mice, *Smad7*^{Cre} is also present in the endothelial cells lining the dorsal aorta (Fig. 1j). Although more restricted, this *Smad7*^{Cre} cardiovascular expression pattern is analogous to that observed with *Tie2*^{Cre} mice. *Tie2*^{Cre} mice have proved to be an extremely useful tool for examination of lineage derivatives and the genes expressed within the endothelial cell population, as *Tie2*^{Cre} is expressed in all endothelial cells including the yolk sac (de Lange *et al*., 2004;Kisanuki *et al*., 2001). Thus, the *Smad7*^{Cre} mice represent a useful additional model that exhibits restricted Cre expression in only a subpopulation of the endothelial lineage.

To determine whether the *Smad7*^{Cre} *lacZ*-positive cells are those that undergo EMT to populate the cushion or they are the cells that do not undergo this transition, we used genetic cell ablation. *Smad7*^{Cre} mice were crossed to *ROSA26*$^{eGFP\text{-}DTA}$ (*R26*^{DTA}) mice (Ivanova *et al*., 2005) to determine the functional role of the *Smad7*^{Cre} lineage during embryonic cardiovascular morphogenesis. When E10.5 *Smad7*^{Cre}*;R26*$^{-DTA}$ mice were harvested (see Fig. 2), ablated embryos were hemorrhaging and had smaller hearts and hypoplastic branchial arches than control littermates (Fig. 2a–c). There was virtually no vasculature in the yolk sac of the mutants in contrast to that of the control littermates (Fig. 2d,e). As we did not observe any *Smad7*^{Cre}-mediated *lacZ* reporter expression in the yolk sac, the lack of yolk sac vasculature in the mutant is likely, secondary to cardiovascular defects. To assess both cardiomyocyte and vascular smooth muscle cell lineages in ablated hearts, we examined α-smooth muscle actin (α-SMA) protein expression. αSMA marks only the cardiomocytes in the heart at this developmental stage, and the mutant myocardium appeared intact and normal. Additionally, both the ventricular myocardium and endothelial layer was intact, but the AV cushions were extremely hypoplastic (Fig. 2f). At this stage in normal embryos, EMT has initiated and usually the cushions are populated with mesenchyme (Fig. 2g). Instead of the normal large paired dorsal aorta surrounded by vascular smooth muscle (Fig. 2i), the mutant dorsal aorta were fragmented and only a few αSMA-positive cells remained. Because of *Smad7*^{Cre}-mediated endothelial cell ablation, the vessels are weakened and hemorrhaged, resulting in in utero lethality and dysmorphic yolk sac in the mutants.

To verify the efficiency of the DTA-mediated cell ablation, we combined the *R26r* reporter mice with the *Smad7*^{Cre}*;R26*^{DTA} mice and developed a triple transgenic mouse. This enabled us to visualize the *Smad7*^{Cre} expressing cells with the *lacZ* reporter, and to determine how effectively they were genetically ablated following activation of DTA (see Fig. 3). By E10.5, *Smad7*^{Cre}*;R26r;R26*^{DTA} embryos exhibited minimal *lacZ* staining (Fig. 3a,b). After 1 day, only a few *lacZ* cells remained in the arches and limb buds (Fig. 3c,d). Notably, the triple transgenic mutant heart has no AV junction, and absent *lacZ* staining in the malformed ectodermal clefts.

To further characterize the hypoplastic cushion phenotype and the effects of the loss of mesenchymal cushions cells on the surrounding heart, we examined the expression of key molecular markers via immunohistochemistry and in situ hybridization (see Fig. 4). α-SMA staining of E10 ablated hearts revealed normal viable myocardium and an intact endocardium in both the OFT and AV (Fig. 4a,b). Given the mutant hypoplastic phenotype and the significant reduction in endocardial cells that are able to undergone EMT and migrate into the cushions (Fig. 4a), we examined whether the mesenchymal cushion marker *Periostin* was still expressed in the few remaining mesenchymal cushion cells. Periostin is a secreted extracellular matrix protein that marks mesenchymal cells in endocardial cushions following EMT (Snider *et al*.,

2008b). We show that *Periostin* mRNA is still highly expressed in the umbilical connection (where *Smad7^{Cre}* is absent) and is expressed in the remaining mesenchymal cushion cells, but that most *Periostin* expressing cells were ablated by E10 (Fig. 4c,d). To examine whether the intact endocardium in both the mutant OFT and AV continues to be viable, we examined Nfatc1 protein expression. Nfatc1 is a transcription factor present in pro-valve endocardial cells and is expressed exclusively in the endocardium from the initiation of endocardial differentiation (de la Pompa *et al*., 1998;Zhou *et al*., 2005). Nfatc1 is expressed during early EMT, but is downregulated at the initiation of valve leaflet remodeling (Zhou *et al*., 2005). Nfatc1 protein is similarly expressed in both the control and ablated hearts (Fig. 4e,f). This indicates that *Smad7^{Cre}* is mainly expressed within the subpopulation of endocardial cells that undergo EMT, as when they are ablated, there is negligible invasion into the adjacent acellular cardiac cushions. Surprisingly, even though the ablation of *Smad7^{Cre}* results in a failure of the endocardium to undergo EMT, both the endocardium and adjacent myocardium continue to proliferate normally, as evidenced by Ki67 staining (Fig. 4g,h).

Our data suggest that prior to EMT, the endocardial cells express inhibitory Smad7, which renders them competent to undergo EMT in the AV and OFT cushions. Based on these data, we propose that Smad7 is a critical component of the checks and balances needed to regulate TGFβ superfamily signaling within the heart, and that it is expressed in the cushions to insure that TGFβ signaling is maintained at a consistent threshold to direct EMT during early stage valvulogenesis. This *Smad7^{-Cre}* transgenic line should thus prove useful for genetic analysis of diverse aspects of cardiovascular morphogenesis and as a restricted endocardial cushion lineage deletor line.

MATERIALS AND METHODS

Generation of Smad7^{Cre} Mice and Mice Tissues

A 4.3 kb *XhoI-HindIII Smad7* promoter fragment (Liu *et al*., 2007) was subcloned into the pBS594-EGFPCre expression vector (Le *et al*., 1999). Following diagnostic verification restriction digests, the linearized construct was given to the IU Transgenic Core facility for microinjection into inbred C3HeB/FeJ zygotes, which were then implanted into the oviducts of pseudopregnant Swiss Webster mice as described (Snider *et al*., 2008a). Forward primer 5′-CATTTGGGCCAGCTAAACAT-3′ and reverse primer 5′-CCCGGCAAAACAGGTAGTTA-3′ were used for genotyping *Smad7^{Cre}* transgenic offspring via PCR using mouse genomic DNA from tail using established protocols (Snider *et al*., 2008a). Two independent lines were generated, and as both had similar *lacZ* reporter distribution patterns the data form only one line is shown.

Both *ROSA26$^{eGFP-DTA}$* (Ivanova *et al*., 2005) and *ROSA26R* (from Jackson Laboratories) indicator mice were intercrossed to *Smad7^{Cre}* offspring and genotyped as described (Snider *et al*., 2008a).

Histological Analysis and X-Gal Staining

Tissue isolation, paraformaldehyde fixation, processing, paraffin embedding, and wholemount staining for β-galactosidase were performed as described (Snider *et al*., 2008a,b). Following wholemount *lacZ* staining, 10-μm serial sections were counterstained with eosin or used for immunohistochemistry with αSMA (dilution 1:5,000, Sigma, St. Louis, MO); NFATc1 (dilution 1:150, Santa Cruz, Santa Cruz, CA); or Ki67 (dilution 1:25, DakoCytomation, Carpinteria, CA). The negative control was normal rabbit serum at 1:150 dilution and positive staining within serial sections was examined using at least three individual E10.5 embryos of each genotype.

In Situ Hybridization

Radioactive in situ hybridization for endogenous periostin expression was performed as described (Lindsley *et al.*, 2007). Both sense and antisense ^{35}S-UTP-labeled probes were used, and specific signal was observed only with hybridization of the antisense probe, in at least three independent embryos of each genotype.

Acknowledgments

The authors thank Dr. Brian Sauer (Stowers Institute) for providing the pBS594 EGFP/Cre fusion vector. They also thank Dr. Yan Chen (Chinese Academy of Sciences) for providing the 4.3 kb *Smad7* enhancer, as well as Drs. Andy Copp and Juan Pedro Martinez-Barbera (Institute of Child Health, UCL) for the *ROSA26*$^{eGFP\text{-}DTA}$ mice.

Contract grant sponsors: Riley Children's Foundation, NIH, T32HL079995 Training Grant, American Heart Association Pre-doctoral Fellowship, Indiana University Department of Pediatrics/Cardiology.

LITERATURE CITED

de Lange FJ, Moorman AF, Anderson RH, Männer J, Soufan AT, de Gierde Vries C, Schneider MD, Webb S, van den Hoff MJ, Christoffels VM. Lineage and morphogenetic analysis of the cardiac valves. Circ Res 2004;95:645–654. [PubMed: 15297379]

de la Pompa JL, Timmerman LA, Takimoto H, Yoshida H, Elia AJ, Samper E, Potter J, Wakeham A, Marengere L, Langille BL, Crabtree GR, Mak TW. Role of the NF-ATc transcription factor in morphogenesis of cardiac valves and septum. Nature 1998;392:182–186. [PubMed: 9515963]

Eisenberg LM, Markwald RR. Molecular regulation of atrioventricular valvulosetpal morphogenesis. Circ Res 1995;77:1–6. [PubMed: 7788867]

Hayashi H, Abdollah S, Qiu Y, Cai J, Xu YY, Grinnell BW, Richardson MA, Topper JN, Gimbrone MA, Wrana JL. The MAD-related protein Smad7 associates with the TGFβ receptor and functions as an antagonist of TGFβ signaling. Cell 1997;89:1165–1173. [PubMed: 9215638]

Imamura T, Takase M, Nishihara A, Oeda E, Hanai J, Kawabata M, Miyazono K. Smad6 inhibits signaling by the TGF-β superfamily. Nature 1997;389:622–626. [PubMed: 9335505]

Ivanova A, Signore M, Caro N, Greene ND, Copp AJ, Martinez-Barbera JP. In vivo genetic ablation by Cre-mediated expression of diphtheria toxin fragment A. Genesis 2005;43:129–135. [PubMed: 16267821]

Kavsak P, Rasmussen RK, Causing CG, Bonni S, Zhu H, Thomsen GH, Wrana JL. Smad7 binds to Smurf2 to form a E3 ubiquitin ligase that targets the TGF β receptor for degradation. Mol Cell 2000;6:1365–1375. [PubMed: 11163210]

Kisanuki YY, Hammer RE, Miyazaki J, Williams SC, Richardson JA, Yanagisawa M. Tie2-Cre transgenic mice: A new model for endothelial cell-lineage analysis in vivo. Dev Biol 2001;230:230–242. [PubMed: 11161575]

Le Y, Miller JL, Sauer B. GFP/cre fushion vectors with enhanced expression. Anal Biochem 1999;270:336–338. [PubMed: 10334854]

Lindsley A, Snider P, Zhou H, Rogers R, Wang J, Olaopa M, Kruzynska-Frejtag A, Koushik SV, Lilly B, Burch JBE, Firulli AB, Conway SJ. Identification and characterization of a novel Schwann and outflow tract endocardial cushion lineage-restricted *periostin* enhancer. Dev Biol 2007;307:340–355. [PubMed: 17540359]

Liu X, Chen Q, Kuang C, Zhang M, Ruan Y, Xu ZC, Wang Z, Chen Y. A 4.3kb Smad7 promoter is able to specify gene expression during mouse development. Biochim Biophys Acta 2007;1769:149–152. [PubMed: 17306381]

Loomis CA, Harris E, Michaud J, Wurst W, Hanks M, Joyner AL. The mouse Engrailed-1 gene and ventral limb patterning. Nature 1996;382:360–363. [PubMed: 8684466]

Luukko K, Ylikorkala A, Makela TP. Developmentally regulated expression of Smad3, Smad4, Smad6 and Smad7 involved in TGF-β signaling. Mech Dev 2001;101:209–212. [PubMed: 11231077]

Massague J, Seoane J, Wotton D. Smad transcription factors. Genes Dev 2005;19:2783–2810. [PubMed: 16322555]

Massague J, Wotton D. Transcriptional control by the TGF-β/Smad signaling System. EMBO J 2000;19:1745–1754. [PubMed: 10775259]

Moustakas A, Souchelnytskyi S, Heldin CH. Smad regulation in TGF-β signal transduction. J Cell Sci 2001;114:4359–4369. [PubMed: 11792802]

Nakajima Y, Yamagishi T, Hokari S, Nakamura H. Mechanisms involved in valvuloseptal endocardial cushion formation in early cardiogenesis: Roles of transforming growth factor (TGF)-β and bone morphogenetic protein (BMP). Anat Rec 2000;258:119–127. [PubMed: 10645959]

Nakao A, Afrakhte M, Moren A, Nakayama T, Christian JL, Heuchel R, Itoh S, Kawabata M, Heldin NE, Heldin CH, ten Dijke P. Identification of Smad7, a TGF-β inducible antagonist of TGF-β signaling. Nature 1997;389:631–635. [PubMed: 9335507]

Schroeder JA, Jackson LF, Lee DC, Camenisch TD. Form and function of developing heart valves: Coordination by extracellular matrix and growth factor signaling. J Mol Med 2003;81:392–403. [PubMed: 12827270]

Snider P, Fix JL, Rogers R, Peabody-Dowling G, Ingram D, Lilly B, Conway SJ. Generation and characterization of Csrp1 enhancer-driven tissue-restricted cre recombinase mice. Genesis 2008a; 46:167–176. [PubMed: 18327771]

Snider P, Hinton RB, Moreno-Rodriguez RA, Wang J, Rogers R, Lindsley A, Ingram DA, Menick D, Field L, Firulli AB, Molkentin JD, Markwald RR, Conway SJ. Periostin is required for maturation and extracellular matrix stabilization of noncardiomyocyte lineages of the heart. Circ Res 2008b; 102:752–760. [PubMed: 18296617]

Snider P, Olaopa M, Firulli AB, Conway SJ. Cardiovascular development and the colonizing cardiac neural crest lineage. Scientific- WorldJournal 2007;7:1090–1113. [PubMed: 17619792]

Soriano P. Generalized lacZ expression with the ROSA26 Cre reporter strain. Nat Genet 1999;21:70–71. [PubMed: 9916792]

Stevens MV, Broka DM, Parker P, Rogowitz E, Vaillancourt RR, Camenisch TD. MEKK3 initiates transforming growth factor β2- dependent epithelial-to-mesenchymal transition during endocardial cushion morphogenesis. Circ Res 2008;103:1430–1440. [PubMed: 19008476]

Zhou B, Wu B, Tompkins KL, Boyer KL, Grindley JC, Baldwin HS. Characterization of Nfatc1 regulation identifies an enhancer required for gene expression that is specific to pro-valve endocardial cells in the developing heart. Development 2005;132:1137–1146. [PubMed: 15689382]

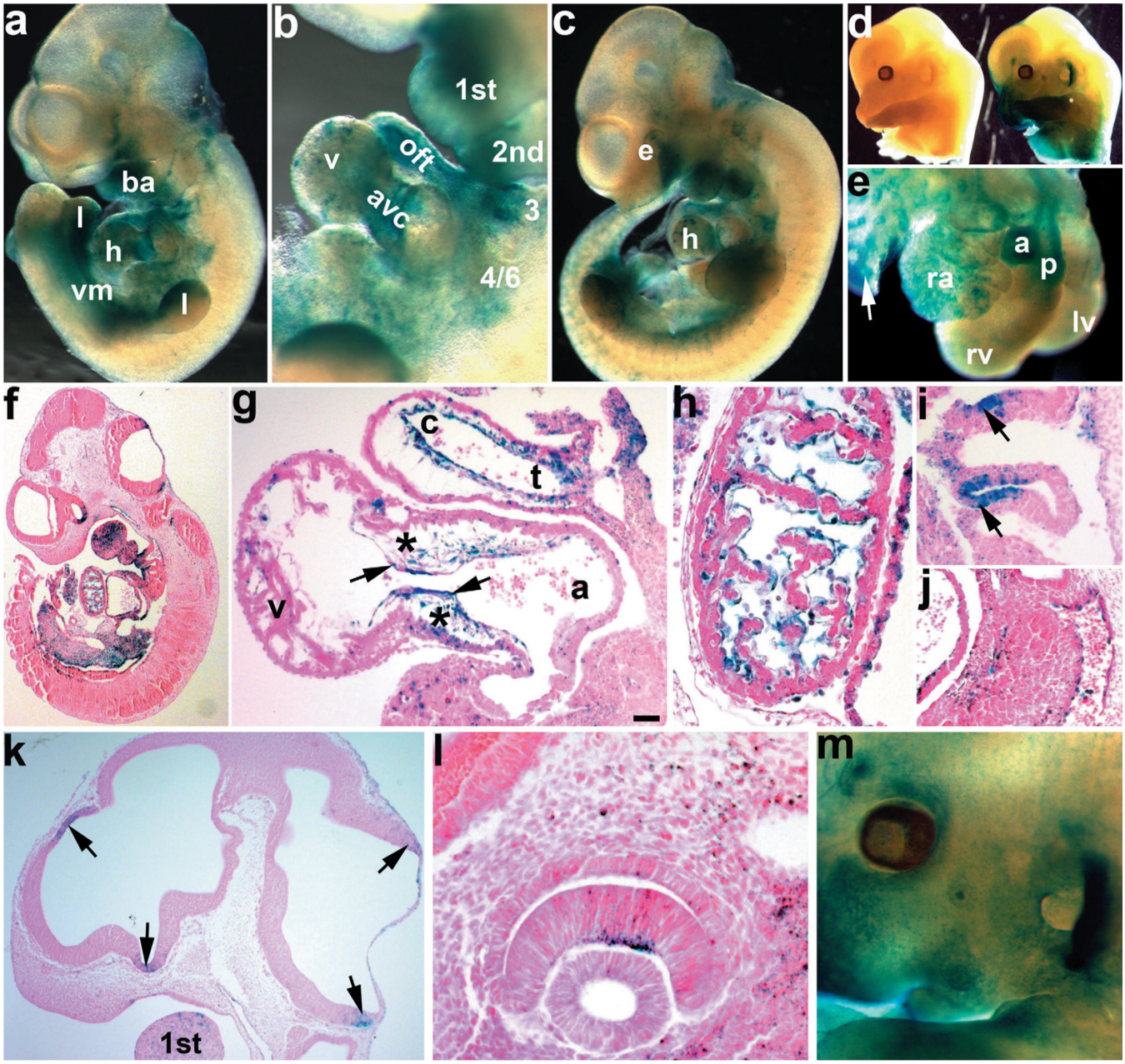

FIG. 1.

Analysis of X-gal stained E10.5 to E13.5 embryos from *Smad7*^{Cre}; *R26r* indicator mice. *Smad7*^{Cre} transgenic males were bred to *R26r* females. Wholemount X-Gal stained embryos were either photographed whole (**a–d, m**), partially dissected to expose heart (**e**), or serially sectioned and counterstained with eosin (**f–l**) to visualize Cre expressing cells. (a) Wholemount *lacZ* stained E10.5 *Smad7*^{Cre};*R26r* embryo. Note *lacZ* expression within the upper jaw, branchial arches (ba), ventral mesenchyme (vm), ventral region of the limb buds (l), and heart (h). (b) Higher magnification view of the first, second, third, and 4/6th branchial arches and heart in a, reveals *lacZ*-expressing cells in the outflow tract (oft) and atrioventricular cushions (avc), and punctate staining in the ventricles (v). (c) E11.5 *Smad7*^{Cre};*R26r* embryo shows more extensive expression in the craniofacial region, the eye (e), arches, heart, and limb buds. (d) E13.5 *lacZ* stained *R26r* only (left) and *Smad7*^{Cre};*R26r* (right) littermate embryos. No

expression is seen in *R26r* only embryos when *Cre* is absent, verifying tissue-restricted reporter expression. (e) Isolated E13.5 heart from *Smad7*^{Cre};*R26r* embryo. Note robust *lacZ* expression in both aorta (a) and pulmonary (p) vessels, as well as punctate *lacZ* in right atria (ra) and left and right ventricles (lv,rv). Also note *lacZ* expression in bronchi of nascent lungs (arrow). (f) Eosin counterstained paraffin section of the embryo in a. (g) Sagittal section of E10.5 *Smad7*^{Cre};*R26r* embryo heart showing robust *lacZ* expression within both the OFT and AV mesenchymal cushions (*) and overlying endocardial cell (arrows) lineages. Note *lacZ* is present within both the conus (c) and truncus (t) of the OFT. (h) E10.5 sagittal section through the myocardium of the heart, note *lacZ* is con- fined to the endocardial cells and absent from the cardiomyocytes. (i) E10.5 sagittal section through aortic arch arteries, showing robust *lacZ* expression in the ectodermal pouches. (j) E10.5 section through the aorta showing *lacZ* staining is restricted to the endothelium (arrow). (k) Sagittal section of the E11.5 *Smad7*^{Cre};*R26r* embryo in c, showing *lacZ* in the neuroepithelium of the forebrain and hindbrain (arrows) and within the first branchial arch. (l,m) High power section of *lacZ* in E11.5 inner neural layer of the optic cup (l), and low power wholemount view of *lacZ* expression in E13.5 eye and ear (m). Scale bar in g = 20 μm. Abbreviation: v = ventricle.

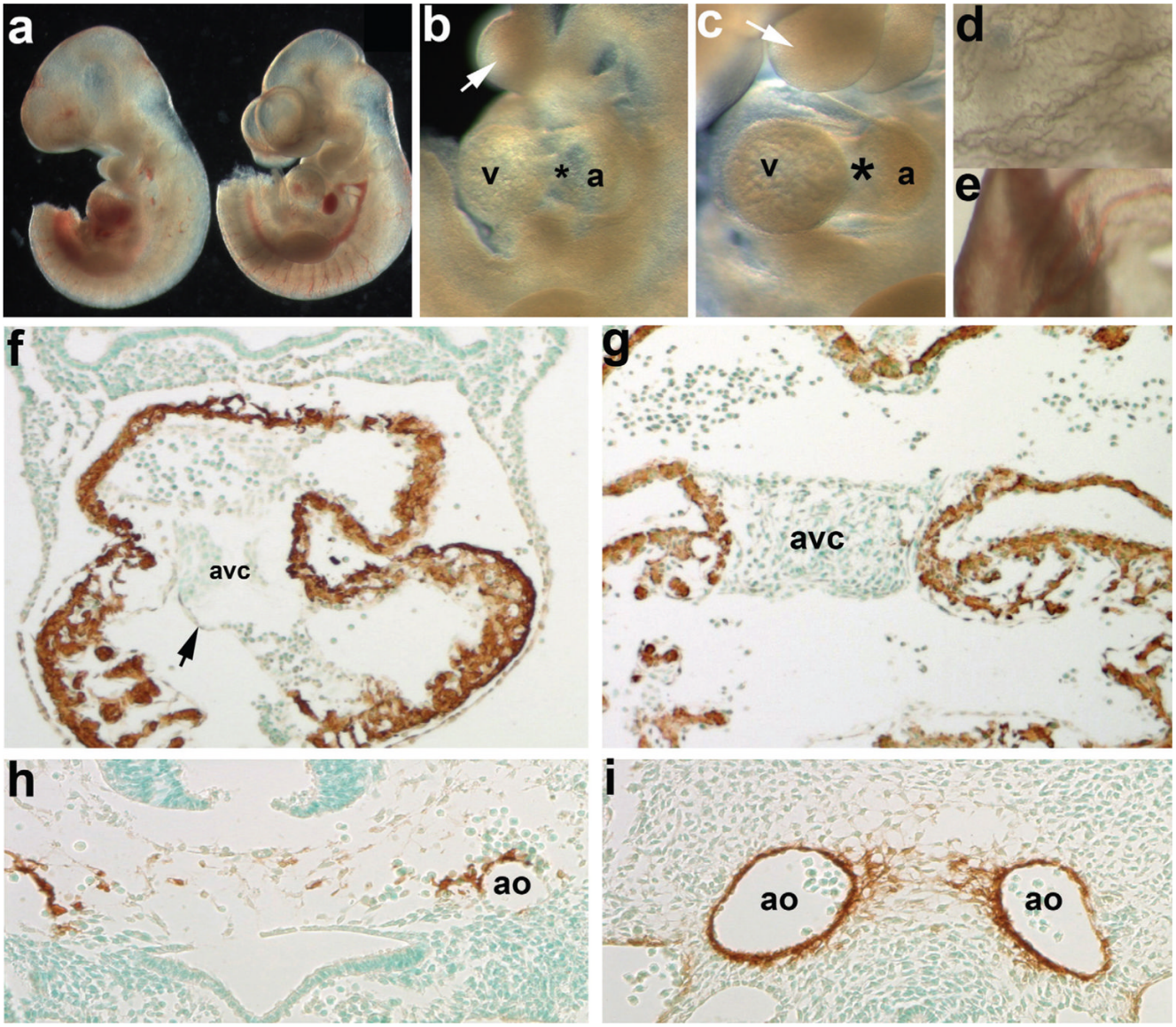

FIG. 2.

Evaluation of resultant cardiovascular phenotypes following Cre/loxP-mediated genetic cell ablation in *Smad7*^{Cre};*R26*^{DTA} embryos. (**a**) E10.5 *Smad7*^{Cre};*R26*^{DTA} (left) and *R26*^{DTA} only (right) embryo littermates. (**b,c**) Higher power images of ablated mutant (b) and normal control (c) cardiovascular and branchial arch regions of embryos shown in a. Note that the AV cushion region (*) is largely absent in mutant (b) hearts and that the arches are smaller in size (arrows). (**d,e**) High power images of the mutant (d) and normal control (e) yolk sacs, note the lack of vasculature and blood in mutant. (**f**) Counterstaining with αSMA (that detects both smooth and cardiac muscle lineages at this stage of in utero development), reveals that the myocardium is largely unaffected via *Smad7*^{Cre}-mediated cell ablation but that the overall size of the heart is decreased, when compared to unaffected littermate photographed at same magnification (**g**). Also note that while the endocardial cushions are hypoplastic, the mutant endothelium remains intact (arrow, g). (**h,i**) α-SMA staining also reveals that whilst the control littermate has two distinct α-SMA-positive paired dorsal aorta (i), and the ablated mutant vessels have hemorrhaged and that there is fragmented α-SMA-stained smooth muscle cells within the mutant (h). Sections f–i were lightly counterstained with methyl green. Abbreviation: a = atria.

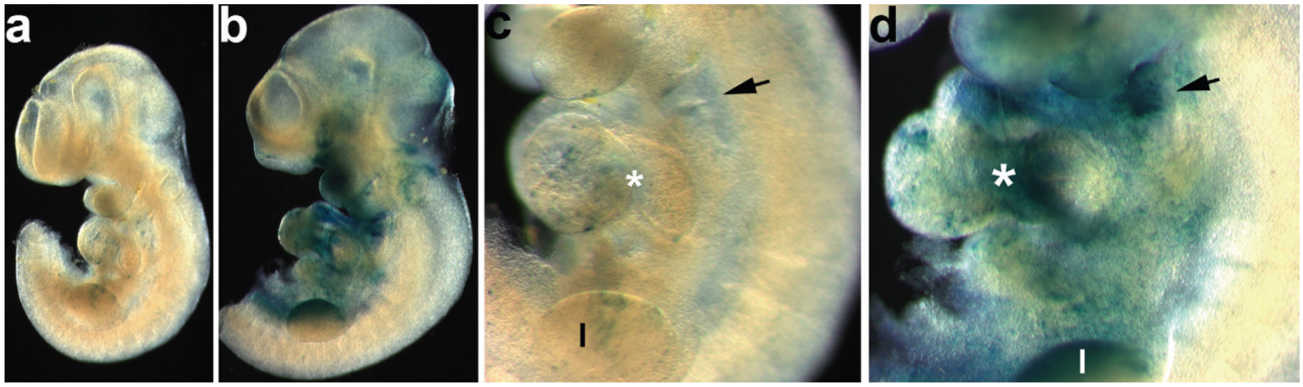

FIG. 3.

Verification of the efficiency of *Smad7*^{Cre}-mediated genetic ablation. *R26r lacZ* reporter mice were crossed with *Smad7*^{Cre} mice and the double transgenics were then bred to *R26*^{DTA} mice, to enable us to visualize in triple transgenic wholemounts how penetrant the genetic cell ablation was. (**a,b**) E10.5 wholemount *lacZ* staining of *Smad7*^{Cre}*;R26*^{DTA}*;R26r* (a) and control *Smad7*^{Cre}*;R26r* only (b) littermates, revealed that most of the *lacZ*-expressing cells had been ablated in triple transgenic mutants when compared to the extensive *lacZ* expression observed in control *Smad7*^{Cre}*;R26r* littermates. (**c,d**) Higher magnification of cardiovascular and branchial arch regions in embryos shown in a and b. Note that in triple mutant transgenic embryos (c), a few *lacZ*-expressing cells can still be detected within the arches, ventricles, and limb buds (l), although in extremely low numbers when compared with the littermate controls (d). Arrows indicate the ectodermal pouches and asterisks indicate the AV canal.

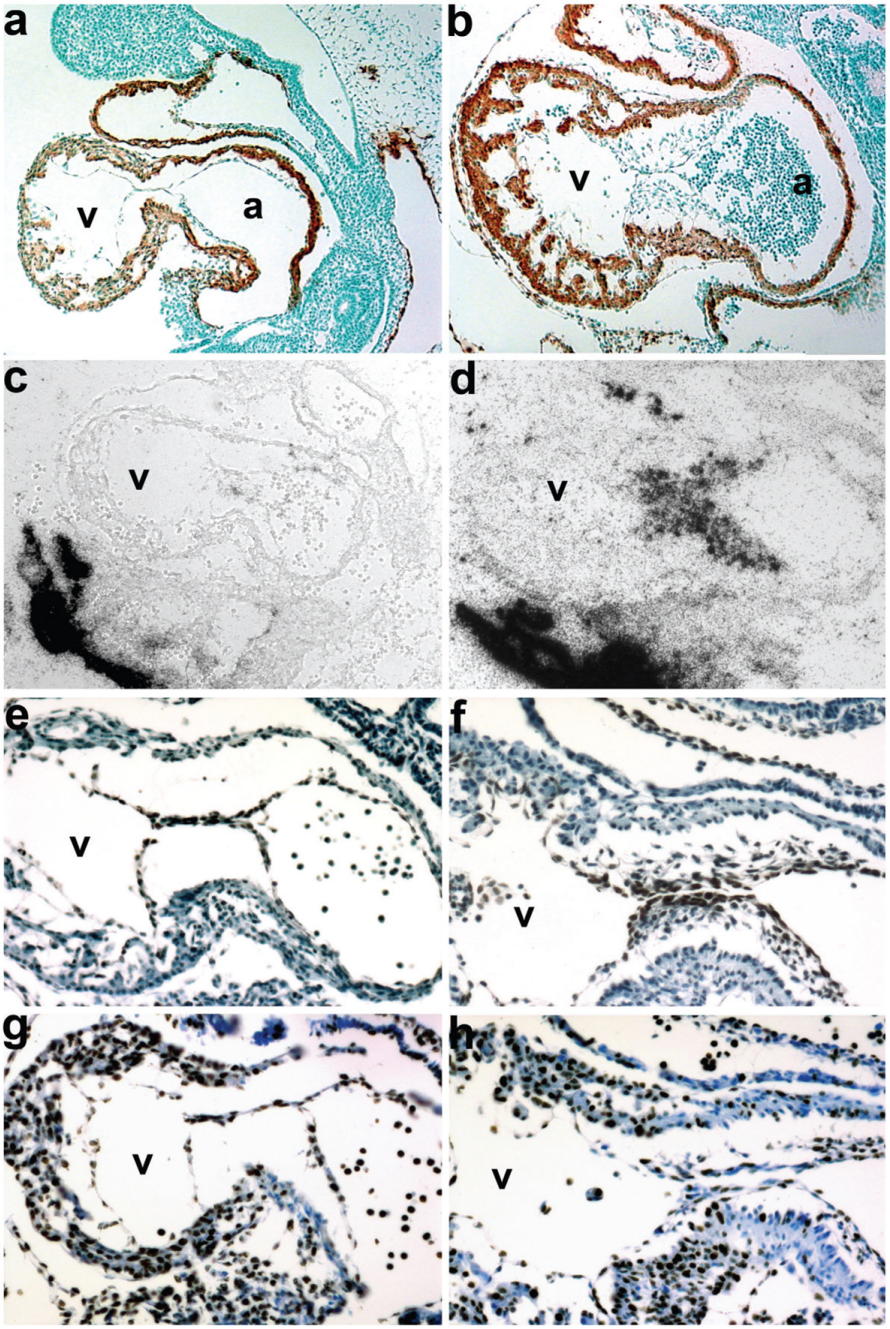

FIG. 4.

Molecular marker analysis of E10 *Smad7*^{Cre};*R26*^{DTA} hypoplastic endocardial cushion phenotype. (**a,b**) Sagittal sections through *Smad7*^{Cre};*R26*^{DTA} (a) and control littermate (b) hearts probed with α-SMA and counterstained with methyl green. Note that the cardiomyocytes within the OFT, ventricle and atria are unaffected; but that the endocardial cushions are absent in ablated mutant hearts. (**c,d**) Radioactive in situ hybridization detection of *Periostin* mRNA in genetically ablated mutant (c) and control (c) embryos reveals very few *Periostin*-expressing cells within the mutant cushions (c). But note robust expression within the mutant umbilical artery and embryonicmaternal connections, which is comparable with control expression levels. (**e,f**) High power views of mutant (e) and control (f) hearts counterstained for Nfatc1

protein. Note that even though the mutant cushions are largely devoid of endocardial cushion cells, Nfatc1 is still expressed within the intact mutant endothelium (e). As expected, unaffected control littermates exhibit both endothelial and cushion Nfatc1 expression (f). (**g,h**) High power views of mutant (g) and control (h) hearts stained for Ki67 protein to assess proliferation. Note the mutant cushion intact endothelial cells and myocardium exhibit comparable proliferation rates as observed in littermate controls (h).